Search for Standard Model Higgs in $H \to \gamma\gamma$ at CMS

Olivier Bondu
on behalf of the CMS collaboration

Institut de Physique Nucléaire de Lyon / Université Claude Bernard Lyon 1

April 16th 2012
Second MCTP Spring Symposium on Higgs Boson Physics
Ann Arbor, MI

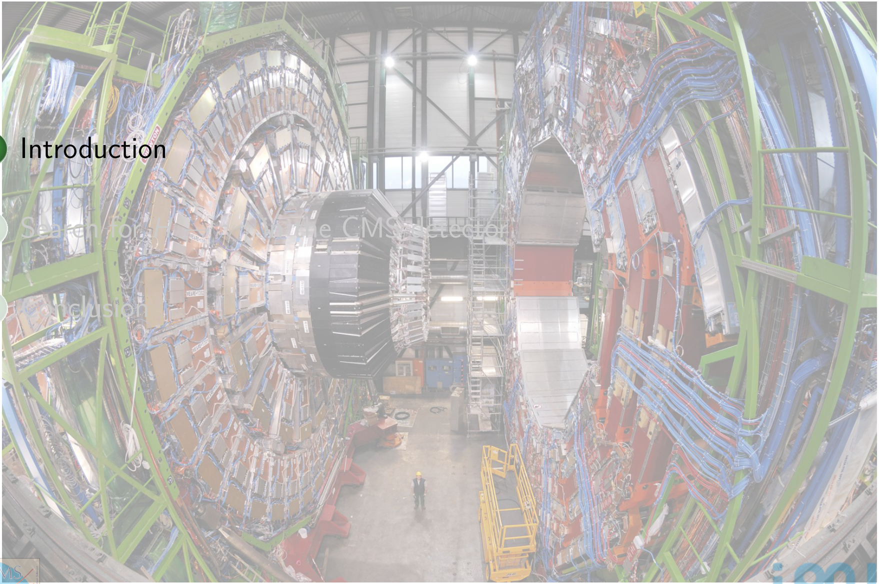

1. Introduction
2. Search for $H \to \gamma\gamma$ in the CMS detector
3. Conclusion

The Higgs boson

http://www.hep.phy.cam.ac.uk/∼wjs/plots/plots.html

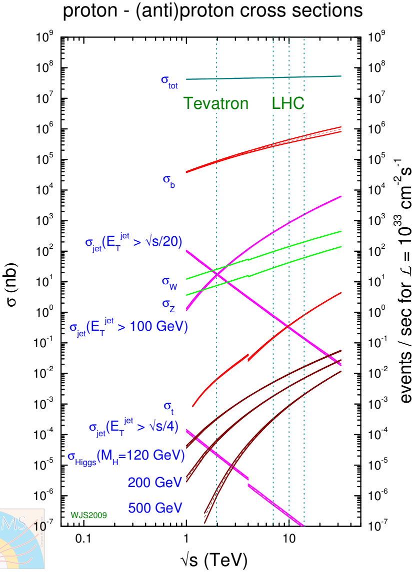

- Relic particle from Higgs mechanism explaining EWSB:
  - Why Z^0 and $W^\pm$ bosons are massive and γ massless?
  - Predicted and observed mechanism: ratio between Z^0 and $W^\pm$ masses, couplings of these bosons to quarks and leptons, ...
- All properties of the Higgs boson are predicted by the Standard Model (couplings, spin, width, ...) except its mass

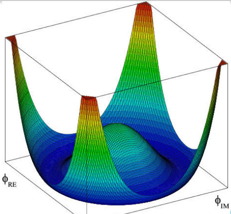

Production of a Higgs boson at the LHC

- The LHC is a hadronic collider: main production channel via gluon fusion

LHC Higgs Cross Section Working Group arXiv:1101.0593

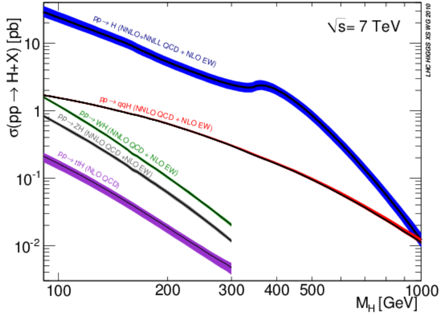

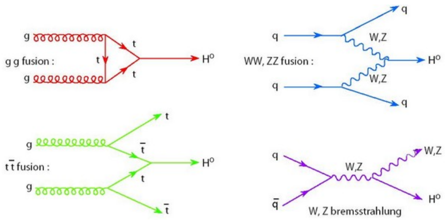

Decay of the Higgs boson

arXiv:1101.0593

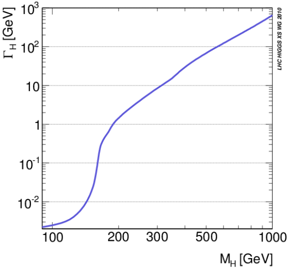

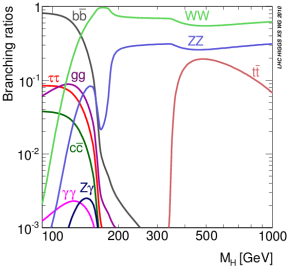

Updated for 2012 Moriond Winter conference,
http://www.cern.ch/LEPEWWG

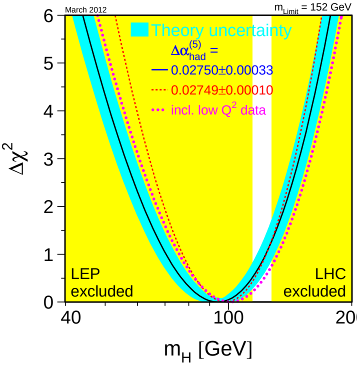

Low mass:

- Favored by EWK precision measurement
- Small decay width
- Decays mainly hadronically (difficult conditions @LHC)

The $H \to \gamma\gamma$ decay channel

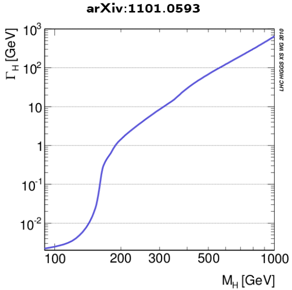

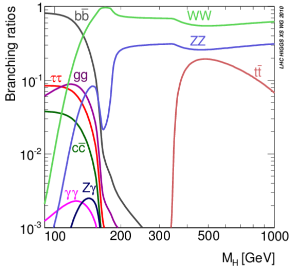

A suppressed decay

- $H \to \gamma\gamma$ branching ratio $\approx 10^{-3}$
- No direct coupling:
  - The Higgs boson is neutral
  - The photon is massless
- Decay possible via loop diagram

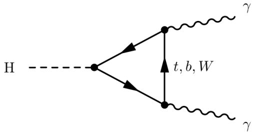

Interest

- Two isolated high-energy photons in the final state
  - Clear and striking signature in hadronic collisions
  - Clean final state topology
  - Small $\Gamma_H \to$ reconstructed invariant mass width ($m_{\gamma\gamma}$) dominated by detector resolution $\to$ peak in invariant mass

The Large Hadron Collider (LHC)

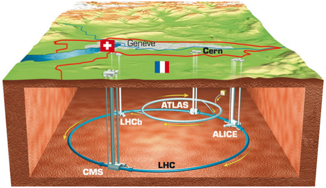

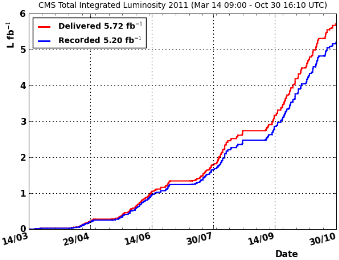

- Proton-proton collider
- Built at CERN, at the France-Switzerland border
- Energy reaching 4 TeV per beam
- 27 km in circumference : 1232 superconducting magnets (1.9 K, up to 8.3 T)
- Bunch crossing every 50 ns
- 10^{14} protons per beam
- Instantaneous luminosity about $4 \times 10^{33}\ \mathrm{cm}^{-2}\mathrm{s}^{-1}$
- Four collision points: CMS is at one of them
- About 5 fb^{-1} of integrated luminosity recorded by CMS at $\sqrt{s} = 7$ TeV

The Compact Muon Solenoid (CMS)

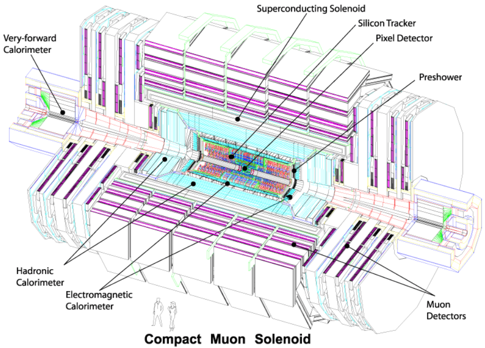

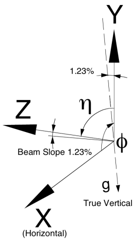

Coordinates

- $\eta = -\ln\left[\tan\left(\frac{\theta}{2}\right)\right]$
- $\Delta R = \sqrt{(\Delta\eta)^2 + (\Delta\phi)^2}$

- One of the two multi-purposes apparati at the LHC
- 28.7 m long, 15 m diameter, weighting 14 000 t
- Superconducting solenoid (3.8 T)
- Compactness : tracker, electromagnetic and hadronic calorimeters within the solenoid
- Several types of muon chambers interleaved with the return yoke

Subdetectors

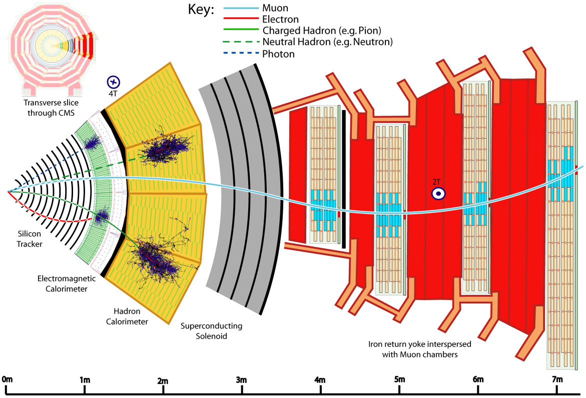

- Pixel detector: determination of the primary vertex of the event
- Silicon tracker: measure transverse momentum of charged particles
- Electromagnetic calorimeter (ECAL): energy of photons and electrons
- Brass/scintillator hadronic calorimeter: (HCAL): energy of hadrons and jets
- Muon chambers: RPC, DT, CSC: muon momentum

Design: fast and dense scintillating crystals

Barrel ↓

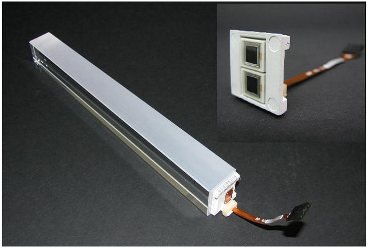

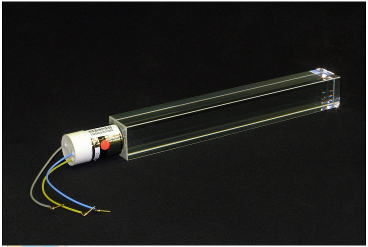

Endcaps ↑

- Scintillating lead tungstate ($PbWO_4$) crystals: high density ($8.28\,g/cm^3$), $X_0 = 0.89\,cm$, Molière radius 2.2 cm
- Collection of scintillation light:
  - Avalanche Photo-Diodes in barrel
  - Vacuum Photo-Triodes in endcaps

- Good resolution (homogeneous crystal)
- Fast: 80 % of scintillation light emitted in 25 ns
- Radiation hard

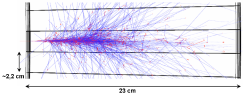

ECAL designed to be fast, compact, radiation-hard with fine granularity and excellent energy resolution

Geometry layout

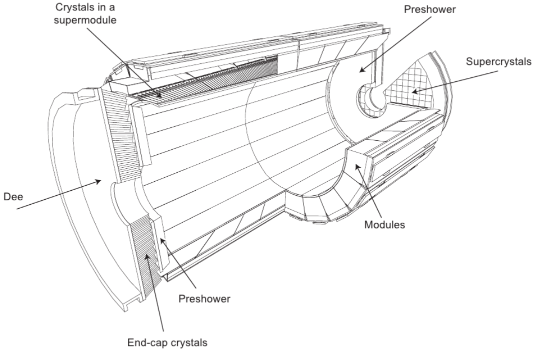

- Central part (EB: ECAL Barrel) composed of 61 200 crystals
- Each endcap (EE : ECAL Endcap) composed of 7 324 crystals
- Crystals (almost) pointing to the interaction point
- Silicon sampling preshower detector (ES : ECAL preShower) for γ / π^0 discrimination
- Material in front of ECAL: about 50 % of photons converts into electron-positron pairs

Energy resolution & laser monitoring

- ECAL energy resolution parametrized in electron test-beams:

$$\frac{\sigma(E)}{E} = \frac{2.8\,\%}{\sqrt{E(\mathrm{GeV})}} \oplus \frac{0.12\,\%}{E(\mathrm{GeV})} \oplus 0.3\,\%$$

stochastic $\oplus$ noise $\oplus$ constant

- For photons of $E \approx 100$ GeV, energy resolution is dominated by the constant term

Goal: constant term $\approx .55\,\%$ during data taking: importance of quality of calibration and monitoring

CMS Collaboration, J. Instrum. 2, (2008), S08004

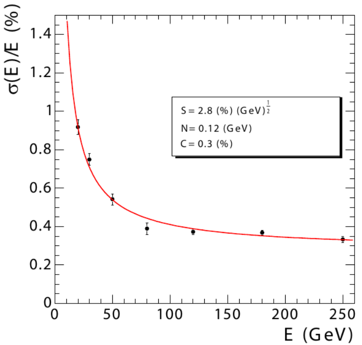

- Transparency loss due to ionisation provoked by radiations → dedicated laser system
- High-voltage and temperature monitoring
- Intercalibration

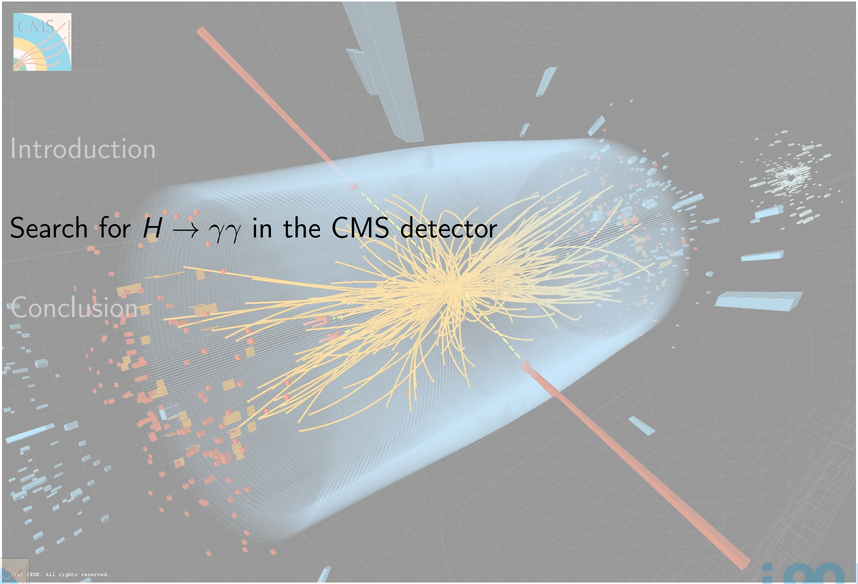

1 Introduction

2 Search for $H \to \gamma\gamma$ in the CMS detector

3 Conclusion

Introduction

Main analysis components:

- Trigger events
- Reconstruct objects: photons, jets
- Identify the right vertex
- Select photons
- Construct event classes by sensitivity
- Model signal and background
- Statistical analysis $\to$ results

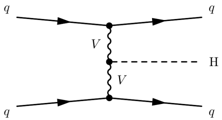

Dijet tag class

- 2 energetic forward jets
- Aimed to select VBF
- Very sensitive
- Disctinct class

Two 'flavors' of the analysis (same dataset):

- Cut-based analysis (baseline arXiv:1202.1487, accepted by PLB)
- Development with multivariate techniques (MVA CMS-PAG-HIG-12-001)

Object reconstruction: photons (1)

Trigger

- Diphoton trigger, with asymmetric E_T tresholds ($\int L = 4.8\,\mathrm{fb}^{-1}$)
- Trigger efficiency studied with $Z^0 \to e^+e^-$ events in data: $> 99\,\%$

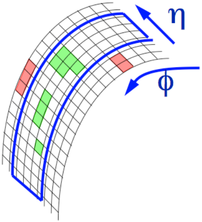

$R_9 = \frac{E_{3\times3}}{E_{SuperCluster}}$ identification of conversions

Energy clustering

- Clusters of energy deposits in ECAL crystals merged into superclusters
- Almost complete recovery of energy of converted photons
  - In barrel: strips of five crystals in η, with extension in ϕ
  - In endcaps: matrices of 5×5 crystals merged along a ϕ-road

Object reconstruction: photons (2)

Energy correction

- Multivariate regression technique (Boosted Decision Tree (BDT)):
  - Trained on simulated sample of photons
  - Input variables: (η_{SC}, ϕ_{SC}) coordinates, shower-shape variables, local cluster coordinates
  - Correct for containment (clustering) and shower losses (conversions)
- Second BDT:
  - Same input variables
  - Provide an estimate of the Gaussian uncertainty on the energy value provided by the first BDT

Vertex location (1)

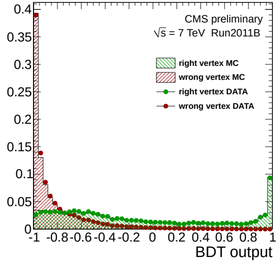

$\epsilon = 83.0 \pm 0.2(\text{stat}) \pm 0.4(\text{syst})$

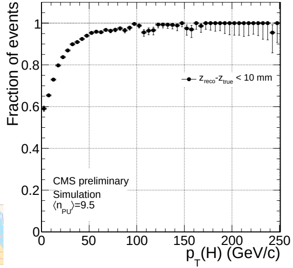

- If $|z_{reco} - z_{true}| < 10$ mm: mass resolution driven by energy resolution

Determination of primary vertex position

Choice of vertex based on BDT:

- No calorimeter pointing
- Input based on kinematic properties:
  $\sum p_T^2 \; ; \; -\sum \left(\vec{p}_T \cdot \frac{\vec{p}_T^{\gamma\gamma}}{|\vec{p}_T^{\gamma\gamma}|}\right) \; ; \; \frac{\sum p_T - p_T^{\gamma\gamma}}{\sum p_T + p_T^{\gamma\gamma}}$
- Input based on photon conversions:
  $\frac{|z_{conv} - z_{vertex}|}{\sigma_{conv}}$
- Efficiency studied with:
  - $Z^0 \to \mu^+\mu^-$ events w/o muon tracks
  - $\gamma +$ jets events

Vertex location (2)

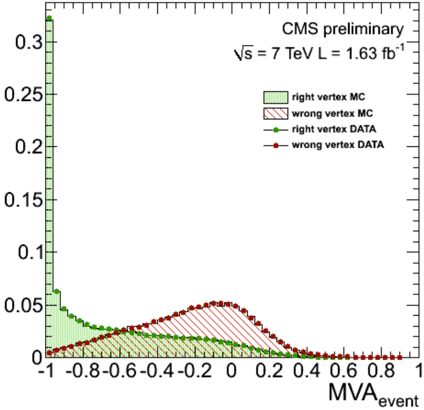

Probability of $|z_{reco} - z_{true}| < 10$ mm (BDT)

- Trained on $H \to \gamma\gamma$
- Inputs:
  - vertex_{BDT} output of the first 3 vertices
  - N_{vtx}, $p_T^{\gamma\gamma}$
  - $|z_{vtx} - z_{2nd}|$ and $|z_{vtx} - z_{3rd}|$
  - N_γ with associated conversion track

Used with photon energy resolution estimate

$\to$ event by event mass resolution

Photon selection (1)

Backgrounds

- 'Irreducible': prompt diphoton
- 'Reducible': $\gamma + jet$ and dijet, where jet(s) misidentified as a photon
- Aim of photon identification: suppress reducible background

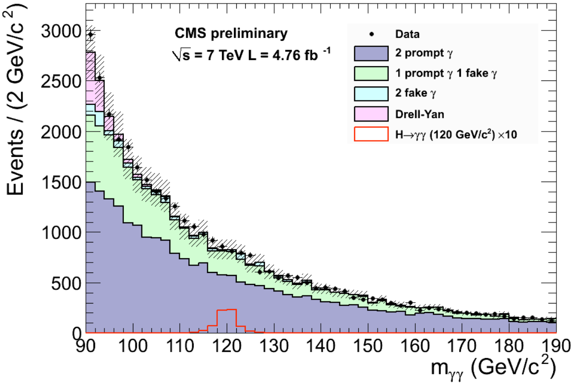

Photon selection (2)

Photon identification, baseline: cut in categories

(Barrel, Endcaps) $\otimes$(low R_9, high R_9): isolation, shower shape, e^--veto

Photon identification, MVA : continuous BDT output

Inputs:
shower shape, isolation, N_{vtx}, η_{SC}

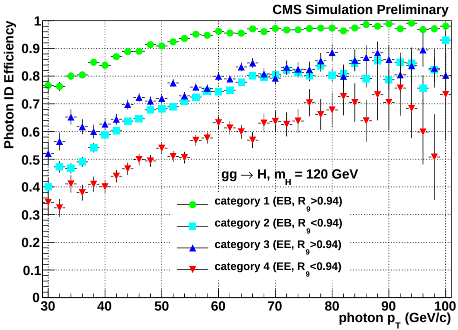

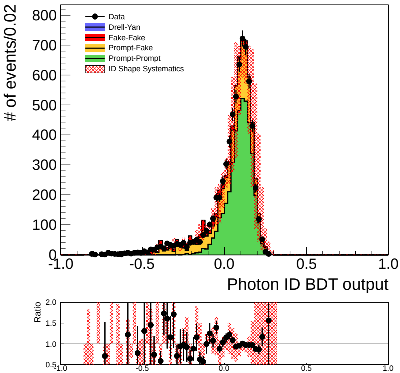

Construction of event classes (1)

Construction of a mass-independent classifier that best scores signal-like kinematics, good photons, good diphoton resolution

Diphoton BDT classifier:

- Photon kinematics: $p_T^{1(2)}/m_{\gamma\gamma}$; $\eta^{1(2)}$; $\cos(\phi_1 - \phi_2)$
- Photon identification:
  - BDT output
- Diphoton mass resolution:
  - $\frac{\sigma_m^{right}}{m_{\gamma\gamma}} = \frac{1}{2}\sqrt{\frac{\sigma_{E_1}^2}{E_1^2} + \frac{\sigma_{E_2}^2}{E_2^2}}$
  - $\frac{\sigma_m^{wrong}}{m_{\gamma\gamma}} = \sqrt{\left(\frac{\sigma_m^{right}}{m_{\gamma\gamma}}\right)^2 + \left(\frac{\sigma_m^{vtx}}{m_{\gamma\gamma}}\right)^2}$
  - $w_{sig} = \frac{p_{vtx}}{\sigma_m^{right}/m_{\gamma\gamma}} + \frac{1-p_{vtx}}{\sigma_m^{wrong}/m_{\gamma\gamma}}$

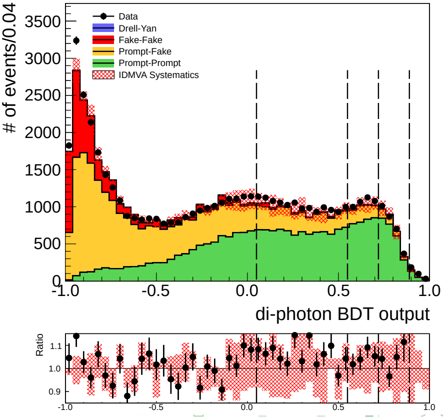

Construction of event classes (2)

Baseline:

- Four resolution classes in R_9^{min} and $|\eta|^{max}$
- One dijet class aimed to select VBF

MVA:

- Four classes in diphoton BDT output
- One dijet class aimed to select VBF

Baseline	Both photons in barrel		One or both in endcap		Dijet
	R_9^{min} >0.94	R_9^{min} <0.94	R_9^{min} >0.94	R_9^{min} <0.94	tag
SM signal expected	25.2 (33.5%)	26.6 (35.3%)	9.5 (12.6%)	11.4 (14.9%)	2.8 (3.7%)
Data (events/GeV)	97.5 (22.8%)	143.4 (33.6%)	76.7 (17.9%)	107.4 (25.1%)	2.3 (0.5%)
σ_{eff} (GeV)	1.39	1.84	2.76	3.19	1.71
FWHM/2.35 (GeV)	1.19	1.53	2.81	3.18	1.37

MVA	0	1	2	3	Dijet tag
SM signal expected	3.4 (4.4%)	19.3 (25.0%)	18.7 (24.2%)	33.0 (42.8%)	2.8 (3.6%)
Data (events/GeV)	4.5 (1.2%)	55.1 (14.8%)	81.3 (21.8%)	229.1 (61.6%)	2.1 (0.6%)
σ_{eff} (GeV)	1.18	1.25	1.64	2.47	1.65
FWHM/2.35 (GeV)	1.09	1.09	1.43	2.08	1.32

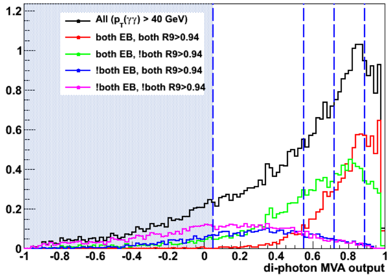

Signal Modelling

Signal

- NLO-Powheg interfaced with Pythia
- For gluon fusion, p_T^H reweighted to (NNLL)+NLO with HqT
- Energy smearing observed in $Z \to e^+e^-$ events data/MC applied

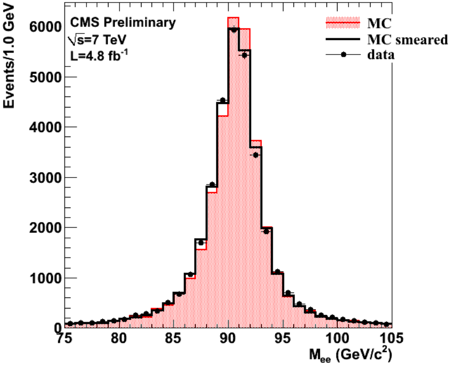

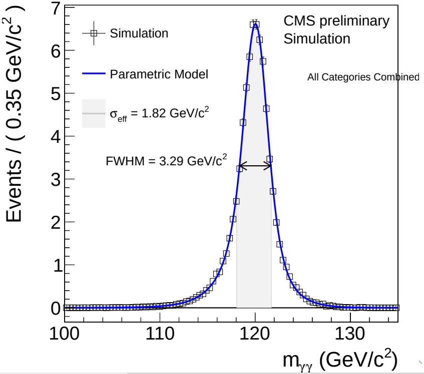

Background modelling (1): baseline

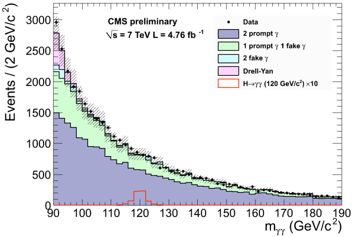

Bias studies

- Toys studies with background only and signal + background
- Choice based on no-bias (correctedness) rather than sensitivity
- Bias (for exclusion or discovery) can be ignored with 5th order polynomial fit

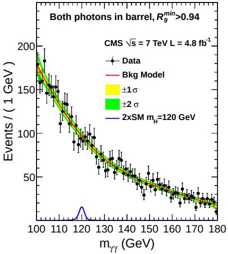

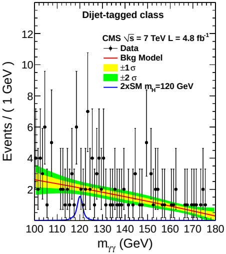

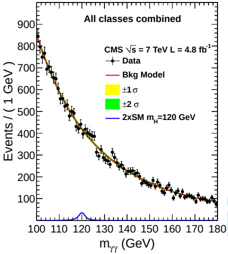

Background modelling (2): MVA, mass fit

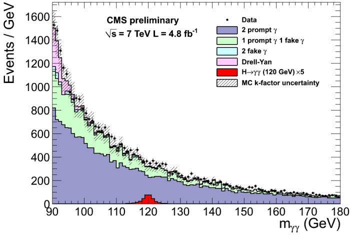

Bias studies

- Toys studies (as before)
- Choice of function / range to limit bias
  - Tested: exponential, power law, polynomial, Laurent series, order raised until no improvement to goodness of fit (F-test)

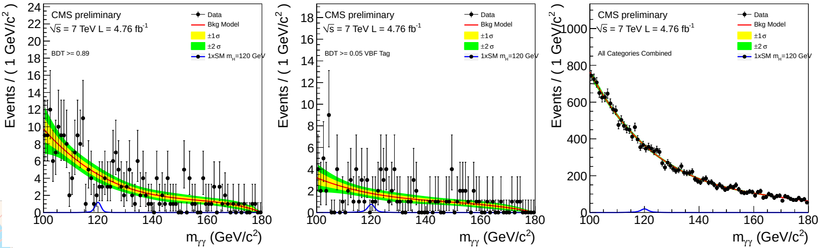

Exclusion limits (1): baseline

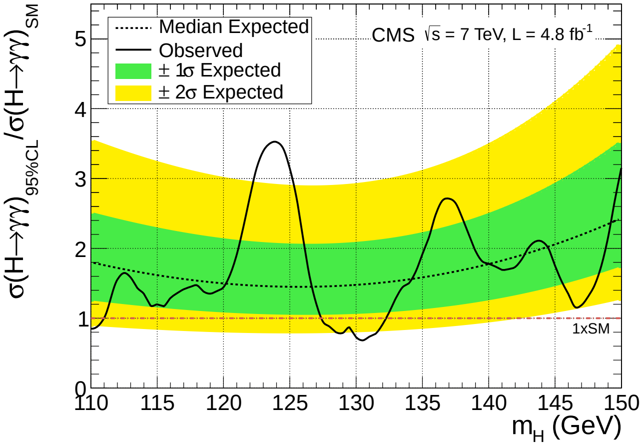

Notes

- Frequentist CL_S computation with unbinned evaluation of the likelihood
- mass range 128 – 132 GeV excluded

Exclusion limits (2): MVA: mass fit

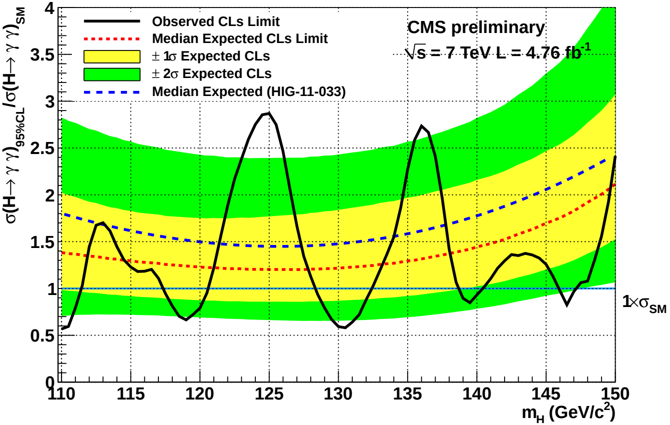

Notes

- Increase of the sensitivity by $\approx 20\,\%$ across the entire masse range
- $110.0 - 111.0$, $117.5 - 120.5$, $128.5 - 132.0$, $139.0 - 140.0$ and $146.0 - 147.0$ GeV excluded
- Cross-checked with BDT fit of mass side bands

Local p-value (1): baseline

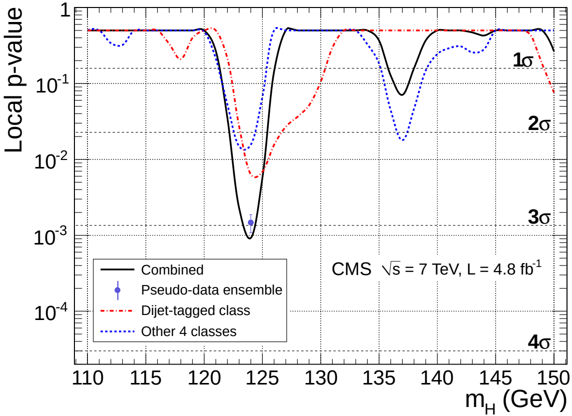

Notes

- Probability for background to produce a fluctuation at least as large as observed
- p-value at 124 GeV of 9.2×10^{-4} ($3.1\,\sigma$) (pseudo-data: $1.5 \pm 0.4 \times 10^{-3}$ ($3.0\,\sigma$))
- Look-elsewhere effect in $110 < m_H < 150$ GeV: p-value of 3.9×10^{-2} ($1.8\,\sigma$)

Local p-value (2): MVA: mass fit

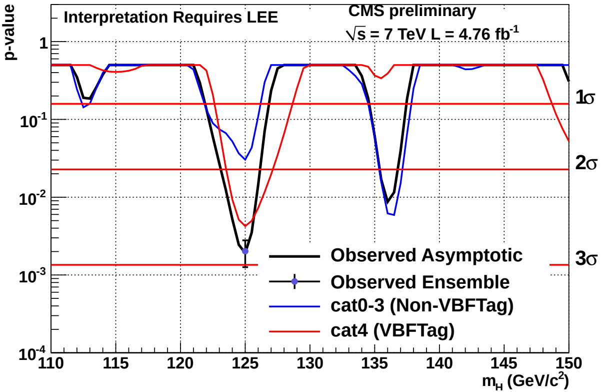

Notes

- Probability for background to produce a fluctuation at least as large as observed
- p-value at 125 GeV of 1.9×10^{-3} ($2.9\,\sigma$) (pseudo-data: $2.0 \pm 0.8 \times 10^{-3}$ ($2.9\,\sigma$))
- Look-elsewhere effect in $110 < m_H < 150$ GeV: p-value of $5.6 \pm 0.4 \times 10^{-2}$ ($1.6\,\sigma$)

Conclusion & Outlook (1)

Conclusion

- Baseline:
  - Sensitivity: $1.4 - 2.4 \times \sigma_H^{SM}$
  - $128 - 132$ GeV range excluded
  - Excess of events @ 124 GeV: local (global) significance of $3.1\,\sigma$ $(1.8\,\sigma)$
- MVA:
  - Sensitivity increased by about 20 %: $1.2 - 2.1 \times \sigma_H^{SM}$
  - $110.0 - 111.0$, $117.5 - 120.5$, $128.5 - 132.0$, $139.0 - 140.0$, $146.0 - 147.0$ GeV excluded
  - Excess of events @ 125 GeV: local (global) significance of $2.9\,\sigma$ $(1.6\,\sigma)$

Conclusion & Outlook (1)

Conclusion

- Baseline:
  - Sensitivity: $1.4 - 2.4 \times \sigma_H^{SM}$
  - $128 - 132$ GeV range excluded
  - Excess of events @ 124 GeV: local (global) significance of $3.1\,\sigma$ $(1.8\,\sigma)$
- MVA:
  - Sensitivity increased by about 20 %: $1.2 - 2.1 \times \sigma_H^{SM}$
  - $110.0 - 111.0$, $117.5 - 120.5$, $128.5 - 132.0$, $139.0 - 140.0$, $146.0 - 147.0$ GeV excluded
  - Excess of events @ 125 GeV: local (global) significance of $2.9\,\sigma$ $(1.6\,\sigma)$

More data needed to ascertain the origin of the excess

Conclusion & Outlook (2)

Outlook

Conclusion & Outlook (2)

Outlook

- We are NOT as naive as one year ago
    - Blinding policy of Higgs searches
        - freeze of analysis techniques
        - deterministic smearing of photon energies ...
-
    -
        -
-

Conclusion & Outlook (2)

Outlook

- We are NOT as naive as one year ago
  - Blinding policy of Higgs searches
    - freeze of analysis techniques
    - deterministic smearing of photon energies ...
- Looking forward to $\approx 15\,\mathrm{fb}^{-1}$ of additional data at $\sqrt{s} = 8$ TeV
  - Should bring an answer to the origin of an excess
    - fluctuation? signal? non-SM like? properties?
-

Conclusion & Outlook (2)

Outlook

- We are NOT as naive as one year ago
  - Blinding policy of Higgs searches
    - freeze of analysis techniques
    - deterministic smearing of photon energies ...
- Looking forward to $\approx 15\,\mathrm{fb}^{-1}$ of additional data at $\sqrt{s} = 8$ TeV
  - Should bring an answer to the origin of an excess
    - fluctuation? signal? non-SM like? properties?
- Impressive re-start of the LHC: $> 650\,\mathrm{pb}^{-1}$ in the last 10 days @8 TeV.....

Stay tuned!

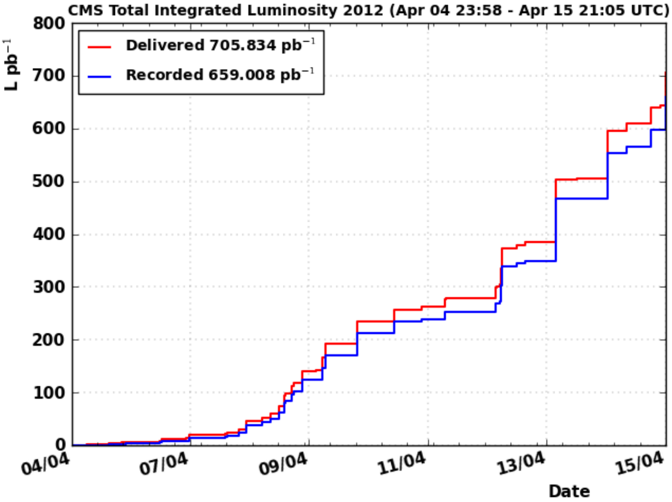

https://twiki.cern.ch/twiki/bin/view/CMSPublic/LumiPublicResults

BACKUP

Best fit signal strength (1): baseline

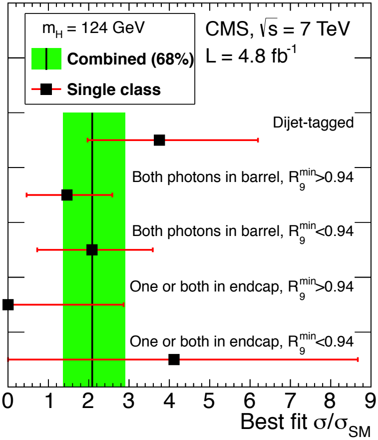

Notes

- Best fit signal strength @$m_H = 124$ GeV: 2.1 ± 0.6 the SM Higgs boson cross section

Best fit signal strength (2): MVA

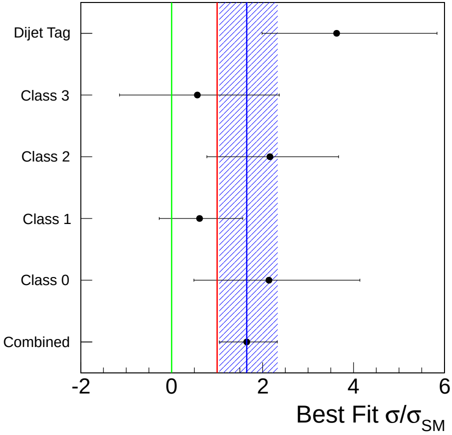

Notes

- Best fit signal strength @$m_H = 125$ GeV: $1.65^{+0.67}_{-0.60}$ the SM Higgs boson cross section

Background modelling (3): MVA, mass side bands

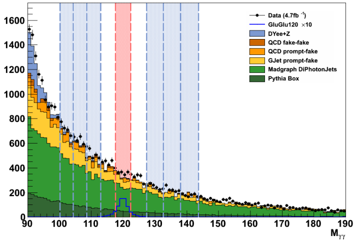

Fit of BDT output

- inputs: diphoton MVA output and $(m_{\gamma\gamma} - m_H)/m_H$
- Assumes fraction of events is linear VS $m_{\gamma\gamma}$
- Less sensitive to parametric form used to describe $m_{\gamma\gamma}$ spectrum

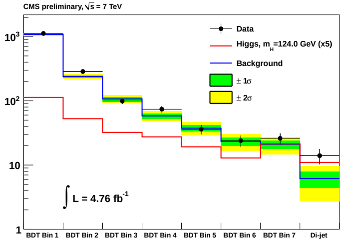

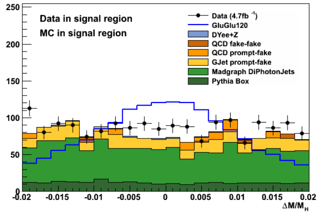

Exclusion limits (3): MVA: mass side bands

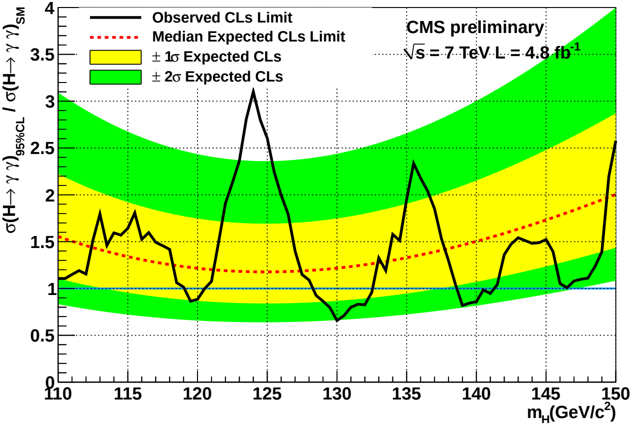

Notes

- Cross-check of the results obtained with mass fit background model
- Larger fluctuations due to events entering and leaving the signal region when mass hypothesis is changed

Local p-value (3): MVA: mass side bands

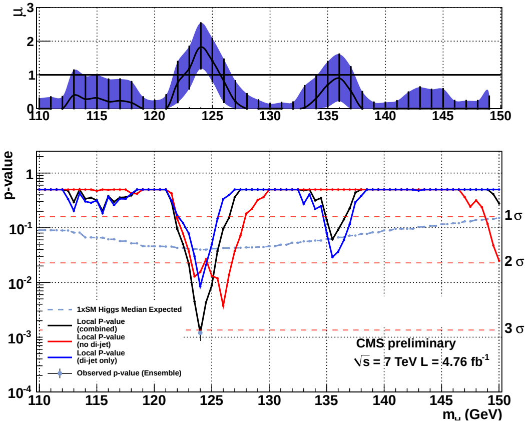

Notes

- Probability for bg to produce a fluctuation at least as large as observed
- p-value at 124 GeV of 1.2×10^{-3} ($3.0\,\sigma$) (pseudo-data: $1.2 \pm 0.3 \times 10^{-3}$ ($3.0\,\sigma$))
- Look-elsewhere effect in $110 < m_H < 150$ GeV: p-value of $1.9\,\sigma$

Limits

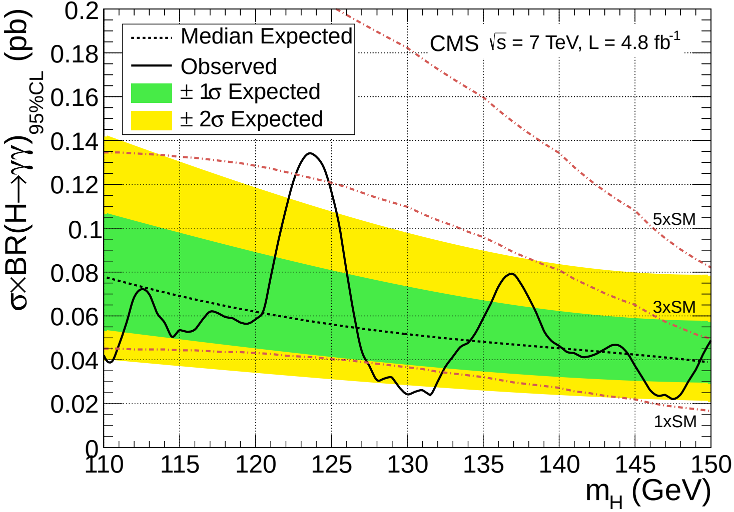
Median Expected
Observed
± 1σ Expected
± 2σ Expected
CMS √s = 7 TeV, L = 4.8 fb-1
5xSM
3xSM
1xSM
σ×BR(H→γγ)95%CL (pb)
0.2
0.18
0.16
0.14
0.12
0.1
0.08
0.06
0.04
0.02
0
110
115
120
125
130
135
140
145
150
mH (GeV)

p-values

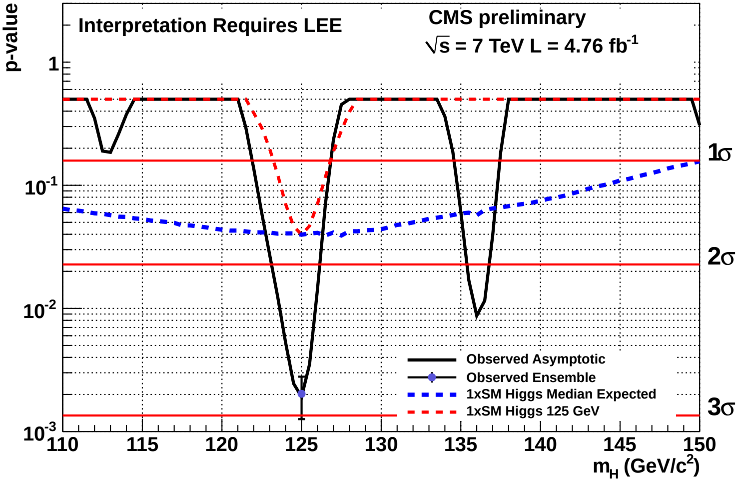

Interpretation Requires LEE
CMS preliminary
√s = 7 TeV L = 4.76 fb-1
p-value
1
10-1
10-2
10-3
110
115
120
125
130
135
140
145
150
mH (GeV/c2)
1σ
2σ
3σ
Observed Asymptotic
Observed Ensemble
1xSM Higgs Median Expected
1xSM Higgs 125 GeV

p-values

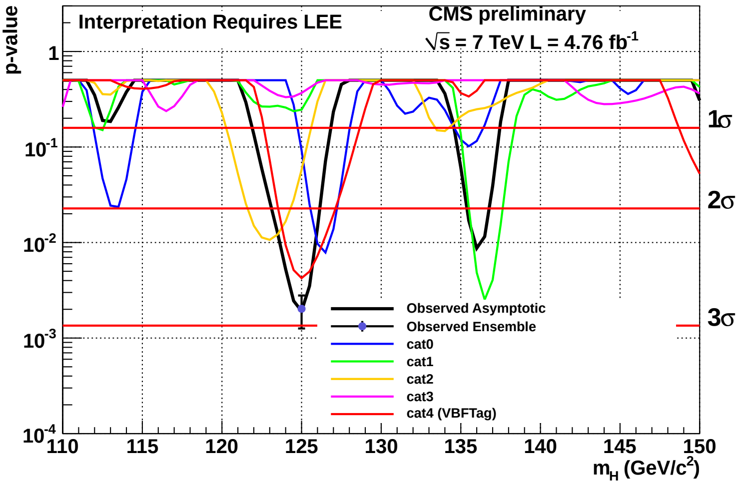
Interpretation Requires LEE
CMS preliminary
$\sqrt{s}$ = 7 TeV L = 4.76 fb^{-1}
p-value
1
10^{-1}
10^{-2}
10^{-3}
10^{-4}
110
115
120
125
130
135
140
145
150
m_H (GeV/c^2)
1σ
2σ
3σ
Observed Asymptotic
Observed Ensemble
cat0
cat1
cat2
cat3
cat4 (VBFTag)

Systematic uncertainties (1): baseline

Sources of systematic uncertainty		Uncertainty	
Per photon		Barrel	Endcap
Photon identification efficiency		1.0%	2.6%
R_9 >0.94 classification (class migration)		4.0%	6.5%
Energy resolution ($\Delta\sigma/E_{MC}$)	$R_9 > 0.94$ (low η, high η)	0.22%, 0.61%	0.91%, 0.34%
	$R_9 < 0.94$ (low η, high η)	0.24%, 0.59%	0.30%, 0.53%
Energy scale ($(E_{data} - E_{MC})/E_{MC}$)	$R_9 > 0.94$ (low η, high η)	0.19%, 0.71%	0.88%, 0.19%
	$R_9 < 0.94$ (low η, high η)	0.13%, 0.51%	0.18%, 0.28%
Per event			
Integrated luminosity		4.5%	
Vertex finding efficiency		0.4%	
Trigger efficiency	One or both photons $R_9 < 0.94$ in endcap	0.4%	
	Other events	0.1%	
Dijet selection			
Dijet-tagging efficiency	VBF process	10%	
	Gluon-gluon fusion process	70%	
Production cross sections		Scale	PDF
Gluon-gluon fusion		+12.5% -8.2%	+7.9% -7.7%
Vector boson fusion		+0.5% -0.3%	+2.7% -2.1%
Associated production with W/Z		1.8%	4.2%
Associated production with $t\bar{t}$		+3.6% -9.5%	8.5%

Systematic uncertainties (2): MVA

Sources of systematic uncertainty		**Uncertainty**	
Per photon		Barrel	Endcap
Photon identification efficiency		1.0%	2.6%
Energy resolution ($\Delta\sigma/E_{MC}$)	$R_9 > 0.94$ (low η, high η)	0.22%, 0.61%	0.91%, 0.34%
	$R_9 < 0.94$ (low η, high η)	0.24%, 0.59%	0.30%, 0.53%
Energy scale ($(E_{data} - E_{MC})/E_{MC}$)	$R_9 > 0.94$ (low η, high η)	0.19%, 0.71%	0.88%, 0.19%
	$R_9 < 0.94$ (low η, high η)	0.13%, 0.51%	0.18%, 0.28%
Photon identification BDT	(Effect of up to 11% event class migration.)	$\pm$0.025 (shape shift)	
Photon energy resolution BDT	(Effect of up to 8% event class migration.)	$\pm$10% (shape scaling)	
Per event			
Integrated luminosity		4.5%	
Vertex finding efficiency		0.4%	
Trigger efficiency	One or both photons $R_9 < 0.94$ in endcap	0.4%	
	Other events	0.1%	
Dijet selection			
Dijet-tagging efficiency	VBF process	10%	
	Gluon-gluon fusion process	70%	
Production cross sections		Scale	PDF
Gluon-gluon fusion		+12.5% -8.2%	+7.9% -7.7%
Vector boson fusion		+0.5% -0.3%	+2.7% -2.1%
Associated production with W/Z		1.8%	4.2%
Associated production with $t\bar{t}$		+3.6% -9.5%	8.5%
Scale and PDF uncertainties	(Effect of up to 16% event class migration.)	(y, p_T)-differential	

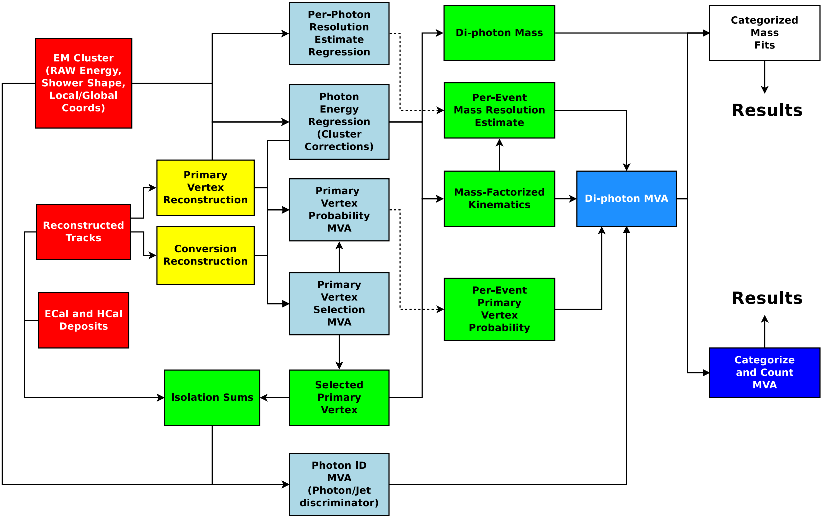
EM Cluster (RAW Energy, Shower Shape, Local/Global Coords)
Per-Photon Resolution Estimate Regression
Photon Energy Regression (Cluster Corrections)
Di-photon Mass
Per-Event Mass Resolution Estimate
Categorized Mass Fits
Results
Primary Vertex Reconstruction
Reconstructed Tracks
Conversion Reconstruction
Primary Vertex Probability MVA
Mass-Factorized Kinematics
Di-photon MVA
ECal and HCal Deposits
Primary Vertex Selection MVA
Per-Event Primary Vertex Probability
Results
Categorize and Count MVA
Isolation Sums
Selected Primary Vertex
Photon ID MVA (Photon/Jet discriminator)

Trigger

R_9 variable defined as $R_9 = \frac{E_{3\times3}}{E_{SuperCluster}}$, used to identify converted photons

Photon identification at trigger level:

- Requirements on R_9 variable (R9ID)
- Requirements on electromagnetic shower shape and very loose isolation (CaloID)

Diphoton trigger:

- Assymmetric E_T tresholds (at least 10 % lower than final selection)
- Each leg having one complementary photon selection (CaloID or R9ID)
- Integrated luminosity corresponds to 4.8 fb^{-1}
- Trigger efficiency studied with $Z^0 \to e^+e^-$ events in data: $> 99\,\%$ efficiency for events passing the offline selection

From rechits towards particle energy

$$E_{e,\gamma} = F_{e,\gamma}(\eta) \cdot \sum_{cluster\ crystals} G(\mathrm{GeV}/ADC) \cdot S_i(T, t) \cdot c_i \cdot A_i$$

- A_i 'rechit'
- c_i intercalibration constant
- S_i correction for crystal transparency loss T as a function of time t
- G global energy scale
- F energy correction: depends on the particle type, energy, pseudo-rapidity, contains the cluster energy corrections

↓ Energy ↓

- Different physics channels for calibration:
  - ϕ-symmetry of minimum bias events
  - $\pi^0 \to \gamma\gamma$, $\eta \to \gamma\gamma$ decays
  - $J/\Psi \to e^+e^-$ decays
  - E/p ratio of electrons from $W^\pm \to e^\pm\nu$ decays
  - $Z^0 \to e^+e^-$ decays
  - $Z^0 \to \mu\mu\gamma$ decays
- Laser monitoring for crystal transparency loss

Clustering algorithms

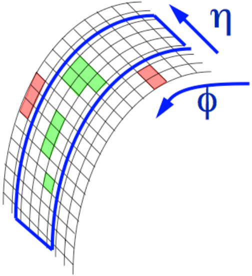

- A particle deposits its energy in several crystals: optimize clustering to give the best energy resolution
  - "hybrid" algorithm in barrel
  - "multi-5x5" algorithm in endcaps
- About 50 % of photons convert in electron-positron pairs, due to material budget
- $R_9 = \frac{E_{3\times3}}{E_{SC}}$ to identify conversions at the cluster level

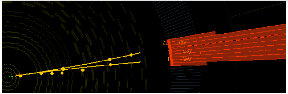

Photon reconstruction and identification at sqrt(s) = 7 TeV (CMS-PAS-EGM-10-005)

Four categories of assignment of the photon energy:

- photon in EB and $R_9 > 0.94$: $E^{\gamma} = E_{5\times5}$
- photon in EB and $R_9 < 0.94$: $E^{\gamma} = E_{hybrid}$
- photon in EE and $R_9 > 0.95$: $E^{\gamma} = E_{5\times5}$
- photon in EE and $R_9 < 0.95$: $E^{\gamma} = E_{multi5\times5}$

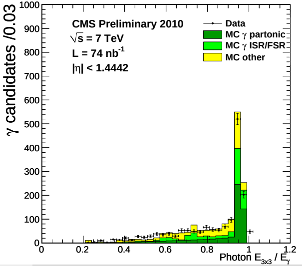

Object reconstruction: jets

Reconstruction of jets

- Particle flow algorithm, considering reconstructed tracks of charged particles and energy deposits in the calorimeters
- Clustering with anti-k_T algorithm with $\Delta R = .5$
- Jet energy measurment calibrated with dijet, $\gamma +$ jets and $Z^0 +$ jets events
- Energy from pile-up and underlying event substracted with FastJet technique

Photon selection (1)

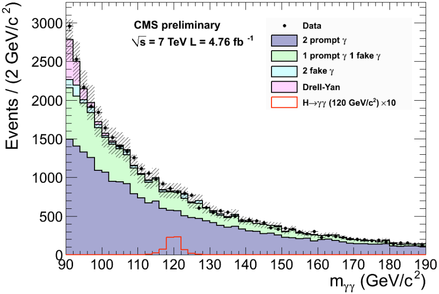

Preselection

- Two photon candidates
- $p_T^\gamma(1) > \frac{m_{\gamma\gamma}}{3}$ and $p_T^\gamma(2) > \frac{m_{\gamma\gamma}}{4}$
- ECAL fiducial region ($|\eta| < 2.5$)
- Excluding transition region $1.44 < |\eta| < 1.57$

Backgrounds

- 'Irreducible': prompt diphoton
- 'Reducible': $\gamma + jet$ and dijet, where jet(s) misidentified as a photon
- Aim of photon identification: suppress reducible background

Photon selection (2)

Photon identification: baseline

Cuts in 4 photon categories (Barrel, Endcaps) $\otimes$ (low R_9, high R_9):

- Isolation cones (PU corrected)
- H/E^{γ}
- Transverse width of electromagnetic shower
- electron veto

Photon identification: MVA analysis

- Preselection
  - electron veto, loose isolation and shower shape cuts
- Training on simulation: signal from $H \to \gamma\gamma$, background from $\gamma +$ jets
- Inputs:
  - Shower topology variables: H/E, $\sigma_{i\eta i\eta}$, R_9, σ_η, σ_ϕ
  - Isolation variables
  - N_{vtx}, η_{SC}

Photon selection (3)

Baseline:

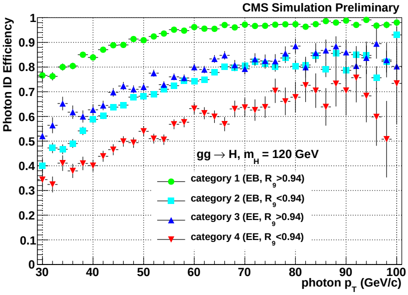

MVA:

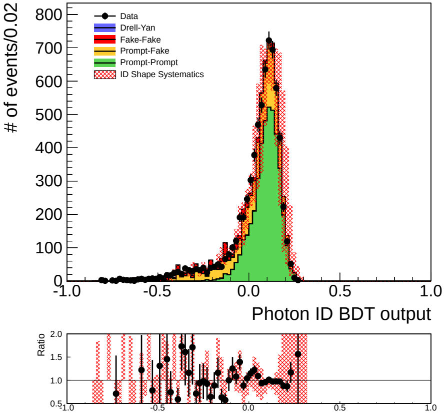

Vertex location (1)

- On average 9.5 p-p interactions per bunch crossing in 2011
- RMS z-spread of 6 cm
- If $|z_{reco} - z_{true}| < 10$ mm: mass resolution driven by energy resolution